Biomedical Materials

PURPOSE-LED PUBLISHING™

PAPER

# Biomimetic and soft lab-on-a-chip platform based on enzymatic-crosslinked silk fibroin hydrogel for 3D cell co-culture

To cite this article: Mariana R Carvalho *et al* 2024 *Biomed. Mater.* **19** 065032

View the article online for updates and enhancements.

You may also like

- Advances on gradient scaffolds for osteochondral tissue engineering
Joaquim M Oliveira, Viviana P Ribeiro and Rui L Reis
- Response of $CO_2$ and $CH_4$ emissions from Arctic tundra soils to a multifactorial manipulation of water table, temperature and thaw depth
K Best, D Zona, E Briant et al.
- Exploring platelet lysate hydrogel-coated suture threads as biofunctional composite living fibers for cell delivery in tissue repair
Raquel Costa-Almeida, Isabel Calejo, Roberta Altieri et al.

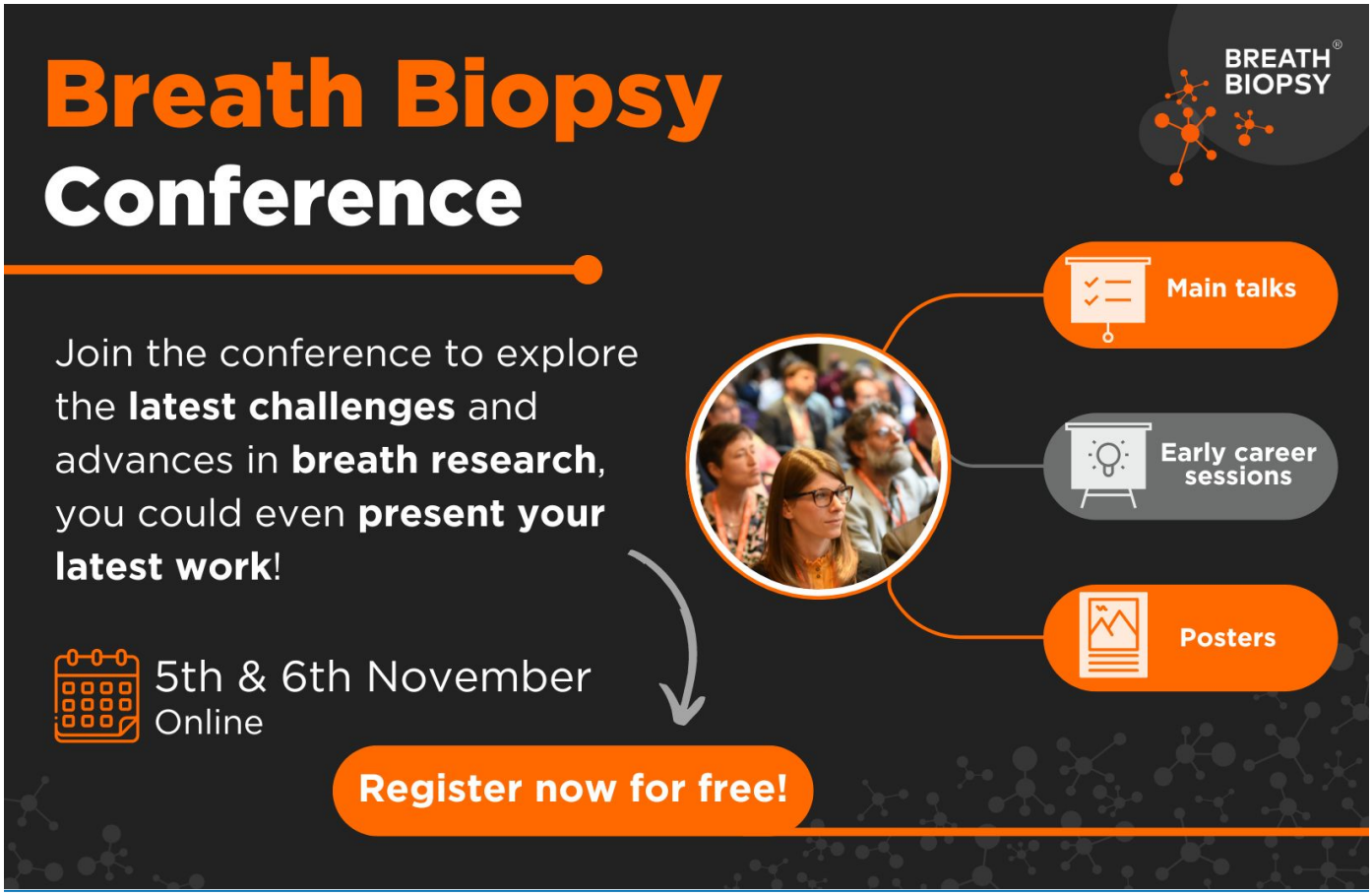


This content was downloaded from IP address 193.137.92.33 on 24/10/2024 at 09:29

Biomedical Materials

PAPER

# Biomimetic and soft lab-on-a-chip platform based on enzymatic-crosslinked silk fibroin hydrogel for 3D cell co-culture

Mariana R Carvalho[1,2], David Caballero[1,2], Subhas C Kundu[1,2], Rui L Reis[1,2] and Joaquim M Oliveira[1,2,*]

[1] 3B's Research Group, I3Bs—Research Institute on Biomaterials, Biodegradables and Biomimetics, University of Minho, Headquarters of the European Institute of Excellence on Tissue Engineering and Regenerative Medicine, AvePark, Parque de Ciência e Tecnologia, Zona Industrial da Gandra, 4805-017 Barco, Guimarães, Portugal
[2] ICVS/3B's—PT Government Associate Laboratory, Braga/Guimarães, Portugal
[*] Author to whom any correspondence should be addressed.

**E-mail:** miguel.oliveira@i3bs.uminho.pt

**RECEIVED**
9 January 2024

**REVISED**
9 October 2024

**ACCEPTED FOR PUBLICATION**
17 October 2024

**PUBLISHED**
24 October 2024

**Keywords:** silk fibroin, microfluidics, enzymatic crosslinking, hydrogel, colorectal cancer model

Supplementary material for this article is available online

## Abstract

Integrating biological material within soft microfluidic systems made of hydrogels offers countless possibilities in biomedical research to overcome the intrinsic limitations of traditional microfluidics based on solid, non-biodegradable, and non-biocompatible materials. Hydrogel-based microfluidic technologies have the potential to transform *in vitro* cell/tissue culture and modeling. However, most hydrogel-based microfluidic platforms are associated with device deformation, poor structural definition, reduced stability/reproducibility due to swelling, and a limited range in rigidity, which threatens their applicability. Herein, we describe a new methodological approach for developing a soft cell-laden microfluidic device based on enzymatically-crosslinked silk fibroin (SF) hydrogels. Its unique mechano-chemical properties and high structural fidelity, make this platform especially suited for *in vitro* disease modelling, as demonstrated by reproducing the native dynamic 3D microenvironment of colorectal cancer and its response to chemotherapeutics in a simplistic way. Results show that from all the tested concentrations, 14 wt% enzymatically-crosslinked SF microfluidic platform has outstanding structural stability and the ability to perfuse fluid while displaying *in vivo*-like biological responses. Overall, this work shows a novel technique to obtain an enzymatically-crosslinked SF microfluidic platform that can be employed for developing soft lab-on-a-chip *in vitro* models.

## 1. Background

Biomedical research has increasingly moved towards the design, fabrication and implementation of microfluidic systems to precisely manipulate fluids and biological material [1, 2]. Polydimethyl siloxane (PDMS) has typically been employed in the development of hard microfluidic platforms due to its unique properties, such as high cell compatibility, optical transparency and oxygen permeability [3]. However, PDMS displays serious drawbacks, including limited mechanical and biochemical properties and degradability that threaten the clinical applicability of PDMS-based devices. To solve this, softer biodegradable materials, such as natural hydrogels, are an excellent alternative to building microfluidic systems (*i.e.* soft microfluidics) [4, 5]. The improvement of soft microfluidics such as the one developed herein present some important features over the hard microfluidics (PDMS), e.g. physiological relevance, functional space, flexibility, ECM interaction analysis, optical properties and easy manipulation. Typical hydrogels include collagen, gelatin, gelatin methacrylate, agarose and alginate, all of them cell-compatible, enabling better interfaces and cell adhesive moieties [6, 7]. Similarly, synthetic hydrogels have been employed to build microfluidic chips [5, 8].

The integration of microfluidic technologies with tissue engineering strategies, such as engineered functional biomaterials as ECM surrogates, is on the

© 2024 IOP Publishing Ltd. All rights, including for text and data mining, AI training, and similar technologies, are reserved.

rise [2]. This combination can efficiently improve the drug discovery pipeline, diagnostics, ameliorate tissue (disease) models, and tissue regeneration processes [9, 10]. Nevertheless, the stiffness of traditional hydrogels is limited when compared to the wide range of human tissues [11], limiting their utility in mimicking physiological condition. Additionally, the degradability of most of these hydrogels is far from desired. Recently, new biomaterials, such as silk fibroin (SF), have been employed in tissue engineering [12]. SF is an FDA-approved material for certain medical applications, gaining a lot of attention in the biomedical field due to its excellent mechanical and biochemical properties [10, 13]. Together with its unique biocompatibility, flexibility, tunable degradability, mild processing conditions, and the presence of accessible chemical groups for functional modifications, SF is an ideal biomaterial for the development of biocompatible microfluidic systems with implantable potential [14, 15]. Notably, SF has already been used in soft microfluidics [11]. Bettinger *et al* [16], reported the fabrication of microfluidic devices made by laminating water-stable micro-molded SF membranes in $\beta$-sheet, which were then modified with macroscopic fluidic connections. However, SF hydrogels in $\beta$-sheet lack the transparency and friendly cellular habitat needed for microfluidic applications [17].

A novel class of enzymatic-crosslinked SF (eSF) hydrogels has recently been reported. Still, being its exploitation limited to engineering *in vitro* 3D static models of disease, bioinks, and as conduits for peripheral nerve regeneration applications [15, 18]. The horseradish peroxidase (HRP)/hydrogen peroxide ($H_2O_2$) cross-linking approach was proposed by Yan *et al* [19], and it is used in polymers containing phenol group, including tyrosine, tyramine or aminophenol [20]. An advantage of this method is that eSF hydrogel proteins remain in an amorphous state, presenting the opportunity to induce $\beta$-sheet conformation if necessary or naturally shifting after 7–10 d. This high degree of versatility and control makes it ideal for developing soft microfluidic systems.

Herein, we describe the development of a biomimetic eSF hydrogel-based microfluidic platform in the amorphous state with mechanical properties not achievable with $\beta$-sheet conformation [14, 16]. The eSF microfluidic chip remains in unstructured conformation for long periods, demonstrating unprecedented structural stability that allows fluid perfusion. As a proof of concept, we designed a microfluidic model of colorectal cancer (CRC) to investigate and characterize distinctive features of the tumor microenvironment. For this, human colonic microvascular endothelial cells (HCoMECs) were injected within the microfluidic channel displaying a serpentine morphology that aimed to reproduce, in a reductionist manner, the abnormal (tortuous) architecture of the tumor vasculature. Next, HCT-116 CRC cells were encapsulated in the bulk of the microfluidic platform. Finally, to evaluate the performance of this model, Gemcitabine (GEM), a typical chemotherapeutic drug currently being tested to treat patients with advanced CRC [21, 22], was perfused through the microchannel, and cell viability was measured.

The choice to use a CRC model relates to the experience of the group in CRC models [23, 24]. It is clear that a model could benefit from its stretching characteristics, such as lung or cardiac tissues. However, a simplistic model where CRC cells are embedded in ECM (mimicked by the SF hydrogel), next to a tortuous microchannel, mimicking the vasculature, can be suitable to study many processes. However, this paper works as a proof of concept where the innovation relies on the achievement of a microfluidic chip made of SF hydrogel, which is transparent and malleable, and allows cell encapsulation, cell seeding and performance of several relevant assays.

Overall, this enzymatic-crosslinked silk hydrogel microfluidic platform promises new ways of engineering and mimicking tissues and pathological states and culturing *in vitro* under dynamic culture conditions. Drug screening and precision nanomedicine are also targets of this advanced technology.

## 2. Materials and methods

### 2.1. Preparation of silk protein fibroin (SF) solution

The purified SF was prepared as described in Yan *et al* [19]. Briefly, SF was dissolved in lithium bromide (9.3 M), followed by dialysis against distilled water for 48 h before concentrating it using a 20 wt% poly(ethylene glycol) solution.

### 2.2. Enzymatically crosslinked SF hydrogel microfluidic platform

*2.2.1. Fabrication of the microfluidic mold*

Standard UV-photolithography and replica molding were employed to fabricate the mold. Briefly, a microfluidic channel with a serpentine morphology was designed by CAD software (AutoCAD, Autodesk) containing channels of 200 μm in width, mimicking the tortuous morphology of the tumor microvasculature. Next, SU8-2010 photoresine (Microchem) was spin-coated on top of a Si wafer to obtain a thickness of 100 μm. A mask aligner (MDA-400M, MIDAS) was used to UV-irradiate the coated Si wafer, removing the non-exposed areas with SU-8 developer (Michochem). The resulting SU8 mold was silanized with trichloro (1H,1H,2H,2H-perfluorooctyl)silane (TCS; Sigma) by vapor phase for 1 h, and cured at 70 °C for 1 h and replicated in PDMS (10:1 w/w pre-polymer: crosslinker; Sylgard 184 Dow Corning).

After pouring the PDMS, the mixture was degassed in a vacuum chamber and cured at 70 °C for 2 h, resulting in a negative PDMS replica. Next, this mold was $O_2$ plasma-activated, silanized with TCS for 1 h under a vacuum, and replicated again in PDMS (10:1 w/w) to generate the final mold for pouring the eSF solution and obtaining the hydrogel microfluidic chip.

*2.2.2. Fabrication of the enzymatically-crosslinked SF hydrogel microfluidic chip*

Hydrogels were prepared by mixing the concentrated SF solution with PBS 1*x* at appropriate volumes to make the final desired concentrations: 6 wt%, 12 wt% and 14 wt% eSF solutions. To promote gelation, 1 ml of SF solution was mixed with HRP (100 µl) and hydrogen peroxide ($H_2O_2$) (65 µl) solutions at 37 °C, as reported previously [19]. HRP solution (0.84 mg·ml$^{-1}$) and $H_2O_2$ (0.36 wt%) were both prepared in PBS 1*x*. The mixture was then poured on the PDMS mold, degassed carefully in a vacuum chamber for air bubble removal and left to crosslink at 37 °C. The devices were easily detached from the mold due to their elasticity. Bonding to a 12% thin partially crosslinked SF hydrogel flat layer was done to seal the chip. All the steps were performed in sterile conditions.

### 2.3. Cell culture

HCT-116 cells (human colon cancer cell line) were initially obtained from the American Type Culture Collection (USA). Cells were cultured in Dulbecco's modified eagle medium (Gibco, Invitrogen) supplemented with 10% fetal bovine serum (FBS) and 1% penicillin and streptomycin (pen/strep) solution under standard conditions (37 °C, 5% $CO_2$). HCoMECs (Innoprot, Spain) were cultured in an endothelial cell medium with 5% FBS, 1% of endothelial cell growth supplement, and 1% of pen/strep solution. The medium was replaced every 3 d. Subculture of cells was performed before 90% confluence using 0.25% trypsin/EDTA (Gibco) for 5 min at 37 °C. All the assays were done in triplicate.

*2.3.1. Cell seeding*

HCT-116 cancer cells were encapsulated in eSF hydrogel at $10 \times 10^6$ cells ml$^{-1}$ and allowed to crosslink within the PDMS mold in the incubator. After peeling, the eSF hydrogel was bonded to the flat eSF layer, and the microchannel was coated with 10% Matrigel solution for 30 min at 37 °C. HCoMECs ($10 \times 10^6$ cells ml$^{-1}$) were manually injected in the microchannel and left to adhere for 6 h in the incubator. Then, the cells were exposed to a perfusion flow of 8 µl per hour for the entire experiment duration (1, 3 and 7 d).

*2.3.2. Exposure to GEM*

After the establishment of the co-culture model, a solution of 5 µM of GEM (Sigma-Aldrich, Germany) was perfused through the inlet tubing using a glass syringe (SGE Analytical Science) mounted on a Nexus 3000 syringe pump. The experiment was carried out for 7 d.

### 2.4. Characterization

*2.4.1. Mechanical properties*

The 6%, 12%, and 14% eSF hydrogels storage and loss moduli were evaluated using an oscillatory model in a rheometer (Kinexus Prot, Malvern). For each measurement, eSF solution (1 ml) was mixed with HRP (100 µl) and $H_2O_2$ (65 µl), which was poured (100 µl) into circular silicone molds of 8 mm in diameter at 37 °C. After crosslinking, the eSF hydrogels were located into the plate of the rheometer to study. The measurements were conducted at 37 °C ($n = 3$). First stress sweeps (0.1 Hz) were performed to determine LVR for all the tested conditions. Frequency sweeps (0.01–1 Hz) were then performed within the LVR. The values of the elastic modulus (G′) were obtained at a frequency of 0.1 Hz.

*2.4.2. Fourier transform infrared—attenuated total reflection (FTIR-ATR)*

The spectrum of a small portion of eSF hydrogel at 14% was measured by FTIR-ATR spectroscopy at days 1, 3 and 7 (Equinox 55, Bruker Optics Inc., USA) in the range of 500–4500 cm$^{-1}$.

*2.4.3. Scanning electron microscope (SEM)*

Samples were sputter coated with gold and analyzed by SEM (JSM-6010 LV, JEOL, Japan) after critical point drying to completely dry the hydrogel (using $CO_2$) to keep the native structure of the microfluidic features.

*2.4.4. Tensile tests*

To perform tensile strength tests on the 14% eSF microfluidic platform, Instron Series 5543 (Instron, UK) was used. Four ($n = 4$) samples measuring 4.16 mm in width and 11.60 mm in 60 mm height were mounted in the apparatus. Tensile strength was measured during the application of pulling force at 1 mm/minute using a load cell of 50 N.

### 2.5. In vitro *assays*

*2.5.1. Cell seeding*

*2.5.2. ATP quantification*

ATP was measured using CellTiter-Glo Luminescent Cell Viability Assay (Promega, Portugal). The reaction is catalyzed by the enzyme luciferase obtained from the firefly (*Photinus pyralis*) to quantify ATP.

For that, either cell cultured in cell culture flasks or encapsulated in eSF hydrogels were placed in 96-well plates. Then, the analysis was performed following the manufacturer's instructions. Briefly, CellTiter-Glo Reagent agent was added (150 µl) to each well of the 96-well plate and incubated for 10 min at

room temperature to lysate cells. Then, the cell lysate (100 µl) was transferred to the wells of a 96-well white opaque microtiter plate (in triplicate). Results were obtained using the luminometer (Perkin-Elmer, USA). The signal intensity of the samples was measured. Results were obtained as integral relative light units (RLUs). An ATP calibration curve was generated using ATP solutions ranging from 5 to 40 000 cells, and luminescence readings from experimental samples were then extrapolated.

*2.5.3. Live/dead assay*

The viability of HCT-116 cells encapsulated in the eSF hydrogel microfluidic chip was assessed by live/dead assay. For this, at endpoints (day 1 and day 3), a portion randomly cut from the device was washed with PBS (Sigma-Aldrich) and incubated for 40 min with calceín AM (1 mM; live cells in green) and ethidium-homodimer (6 mM; dead cells in red). Microfluidic chips were then imaged using an inverted SP8 confocal microscope (Leica, Germany) using automated acquisition for Z-stack and multi-color channel.

*2.5.4. Investigation of the effect of GEM*

The impact of perfusing 5 µM GEM in the system for 1, 3 and 7 d on HCT-116 cells was assessed in terms of metabolic activity by Alamar blue (AB) assay according to supplier's instructions. After each timepoint, a specific cell culture medium containing 20% v/v AB was added to a recipient covering the entire device. After 4 h of incubation, the fluorescence signal was read at 590 nm (excitation wavelength 530 nm) using a microplate reader (FL 600, Bio-Tek Instruments). After each AB determination, cells were washed and a fresh culture medium was added to continue the culture. Medium with 20% v/v AB was used as a blank.

*2.5.5. Fluorescence characterization*

At day 3, cells were fixed with 4% paraformaldehyde in PBS for 30 min at room temperature and washed again with PBS. Cell permeability was performed with 0.1% Triton X-100 (Sigma-Aldrich) for 15 min at room temperature, followed by washing with PBS. High-affinity filamentous actin probe Alexa Fluor 594 Phalloidin (1:80; Invitrogen) was injected through the channels, let to incubate for 45 min at room temperature, washed with PBS, and then incubated with DAPI (1:100; Invitrogen) diluted in PBS for 20 min at room temperature. The samples were observed in an SP8 confocal microscope (Leica, Germany).

### 2.6. Statistical analysis

Statistical analysis was performed using GraphPad Prism 5.0 software (v5.0a). The nonparametric Mann–Whitney test was used to compare two groups, whereas a comparison between more than two groups was performed using the Kruskal–Wallis test, followed by Dunn's comparison test. A value of $p < 0.05$ was considered statistically significant.

## 3. Results

### 3.1. Preparation of SF solution

After obtaining the silk solution at 20%wt, we decided to test different concentrations of silk hydrogel 6 wt%, 12 wt% and 14 wt% to test our new methodology with the aim of obtaining a microfluidic platform.

### 3.2. Enzymatically crosslinked SF hydrogel microfluidic platform

*3.2.1. Fabrication of the microfluidic mold*

Standard UV-photolithography and replica molding were employed to fabricate the mold. This manuscript novelty relates to fabrication method of microdevices, such as microfluidic devices, comprising a HRP enzymatically crosslinked SF hydrogel, and the methods for fabricating the same, already described in Materials and Methods section.

After testing the aforementioned concentrations, the authors realized that the 14 wt% was the best concentration in terms of malleability and transparency parameters, and could be easily detached from the mold due to their elasticity, unlike other silk concentrations. The devices made were easily detached from the mold due to their elasticity.

Regarding the bonding, a 12% thin partially crosslinked SF hydrogel flat layer was done to seal the chip. All the steps were performed in sterile conditions for experiments with cells.

Importantly, the model was designed to comprise a serpentine channel (figure 1(A)). This design was chosen for HCoMECS seeding, media perfusion, and for the injection of anti-cancer drugs while CRC cells were embedded in the hydrogel. The choice of design was made to mimic simply the native tumor environment, which is characterized by displaying a tortuous vasculature, which also composes a challenge for a microfluidic platform made entirely of a hydrogel. Figures 1(B) and (C) show the procedure to fabricate the eSF microfluidic chip using a combination of microfabrication techniques: photolithography and soft lithography (double replica molding), already patented by the group. SEM images in figure 2(D) demonstrate the eSF hydrogel maintained the microfluidic features with excellent fidelity after the entire fabrication process and crosslinking process

### 3.3. Characterization

*3.3.1. Mechanical properties*

Next, we characterized the eSF hydrogel material in terms of mechanical properties. We first characterized the % of eSF using 6, 12, and 14% eSF. Rheology analysis showed that the higher the concentration of eSF, the higher the G', or the stiffness, as expected. The 6% eSF hydrogel presented a G' of 1963 ± 151 Pa, 12%

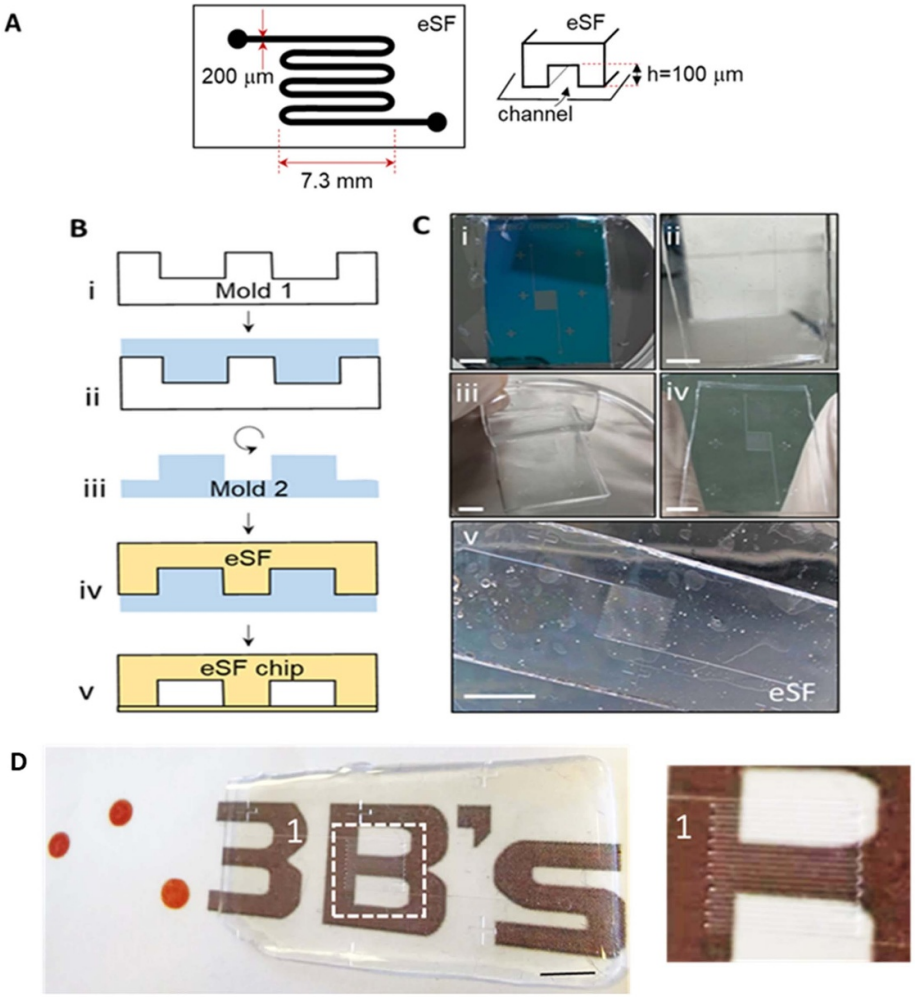


**Figure 1.** Fabrication of the eSF hydrogel based microfluidic chip. (A) Schematic illustration of the eSF microfluidic device, including a serpentine channel. (B) and (C) Scheme and corresponding photographs showing the main steps for fabricating the chip by photolithography and soft lithography (double replica molding): i: SU8 mold 1; ii: PDMS replica; iii–iv: PDMS mold 2; v: eSF chip). (D) Photograph of the eSF chip and the corresponding SEM images of two different areas. (E) Image showing the high degree of transparency of the eSF microfluidic chip and a close up photograph of the serpentine features. Scale bars: 7.3 mm.

eSF hydrogel showed a G' value of 6585 ± 253 Pa, and 14% eSF hydrogel, which gave a G' of 7172 ± 605 Pa (figure 2(A)). The reported results are in agreement with previous results [14]. However, during replica molding, 6 and 12% eSF were significantly brittle, leaving eSF residues in within the PDMS mold channels. They were less transparent than the 14% counterpart. For this reason, 14% eSF hydrogel was selected for building the microfluidic platform and to perform all biological assays.

### *3.3.2. Fourier transform infrared—attenuated total reflection (FTIR-ATR)*

Figure 2(B) shows the ATR-FTIR spectra of silk 14% over 7 d. There is an association between hydrogels network morphology and conformational changes (detected by ATR-FTIR) of the eSF proteins. When incubating the eSF hydrogel (in PBS at 37 °C), a relatively transparent morphology is observed over 7 d, starting to change at day 7 to opaque until 10 d [17]. As shown in the FTIR-ATR spectra (figure 2(B)), where there is a clear shift around 1600 $cm^{-1}$, indicating a protein conformation change from amorphous to $\beta$-sheet (as seen by the green line).

### *3.3.3. SEM*

Since it is not possible to observe wet samples in SEM, and the eSF hydrogel microfluidic platform is in its base, a hydrogel, it was subjected to critical point drying using $CO_2$, in an attempt to maintain its form and be able to be observed under SEM. Indeed, this result is of significance since SEM images reveal that it retains the intricate serpentine features with high level of fidelity. This means that after peeling the hydrogel off the mold, its features no not break or bend (figure 2(D)).

### *3.3.4. Tensile tests*

We next investigated the deformation capacity of the microfluidic chip. For this, we performed tensile tests on the 14% eSF, finding a mean tensile strain of 103.96% (figure 2(C)). This means that the hydrogel

A)

| Formulation | Cells | Incubation time | Storage modulus (G', Pa) | Loss modulus (G", Pa) |
|---|---|---|---|---|
| 6% | no | 30min | 1963±151 | 30±16 |
| 12% | no | 30min | 6585 ± 253 | 152 ± 48 |
| 14% | no | 30min | 7173 ± 605 | 387 ± 64 |
| PDMS | | | 580000 ± 1005 | 3298 ± 174 |

B)

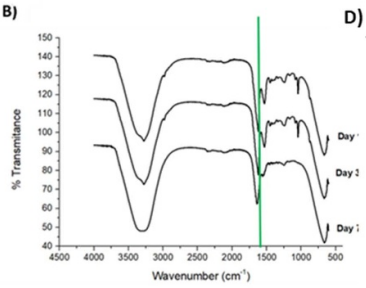


D)

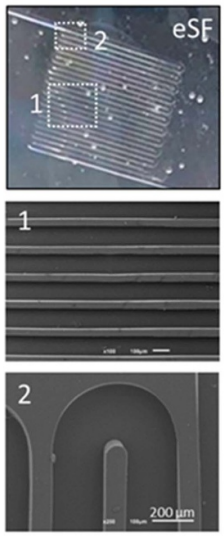


C)

| Tensile Tests of 14% eSF microfluidic platform | |
|---|---|
| Elongation at max force [%] | 103.96 ± 26.8 |
| Tensile stress at Maximum Force [kPa] | 5.46 ± 1 |
| Young's Tensile stress [kPa] | 11.79 ± 1.3 |

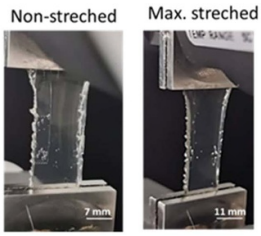


**Figure 2.** Characterization of the eSF microfluidic hydrogel. (A) Oscillatory rheological measurements (frequency 1 Hz) for eSF hydrogels at different concentrations (6%, 12%, and 14%). (B) ATR-FTIR spectra for the 3D eSF hydrogel (with 14% eSF) retaining the amorphous protein structure for at least 7 d. (C) Tensile tests on 14% eSF microfluidic platform and photograph showcasing the high degree of deformation of the eSF hydrogel.

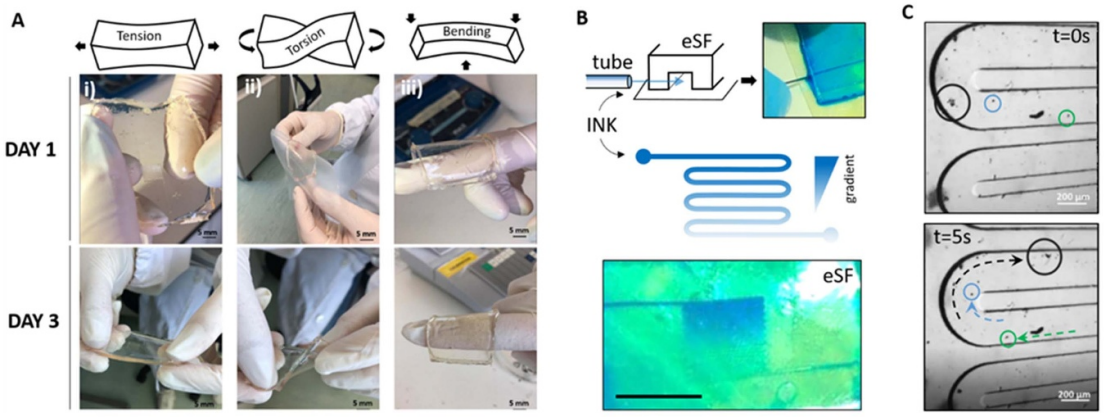


**Figure 3.** Characteristics of the 14% eSF hydrogel microfluidic platform. (A) Images showing the unique mechanical properties of the developed platform after stretching (tension), torsion, and bending at days 1 and 3. (B) Perfusion of blue ink through the serpentine channel and formation of a soluble ink gradient due to the hydrophilic nature of the eSF hydrogel. Scale bar: 7.3 mm. (C) Representative microscopy snapshots showing the flow of microstructures along the serpentine channel.

can be stretched twice its original size. Finally, regarding the Young's modulus, the hydrogels can endure about 11.79 kPa until it breaks.

Next, we evaluated the capability of the eSF chip to recover to other types of mechanical actuation, namely manual tension, torsion, and bending (figure 3(A)). We found that the eSF chip displayed a remarkable flexibility. The chip was stretched, bent, and twisted without breaking or damaging the inner channel for at least 3 d when kept in medium or PBS to avoid dehydration (figure 3(A)). Moreover, since the hydrogel is very hydrophilic, concerns were present at the time of diffusion due to water resistance. However, these were overcome as can be seen by perfusion evidences in figures 3(B) and (C). Moreover, the edges of the device can be seen in the provided video where it is shown that there is no leakage (see supplementary files).

### 3.4. In vitro *assays*

#### *3.4.1. Cell seeding*

We aimed at building a very simplistic colorectal tumor model, as shown in figure 4(A). For this, we encapsulated HCT-116 (CRC cells) within the bulk of the eSF hydrogel and HCoMECS were seeded in the serpentine microchannel, as depicted in schematics. The seeding was successful and was followed by more in depth analysis.

#### *3.4.2. Fluorescence characterization*

Figure 4(B) focuses on the culture and adhesion of HCoMECS on the eSF microchannel. Cells showed

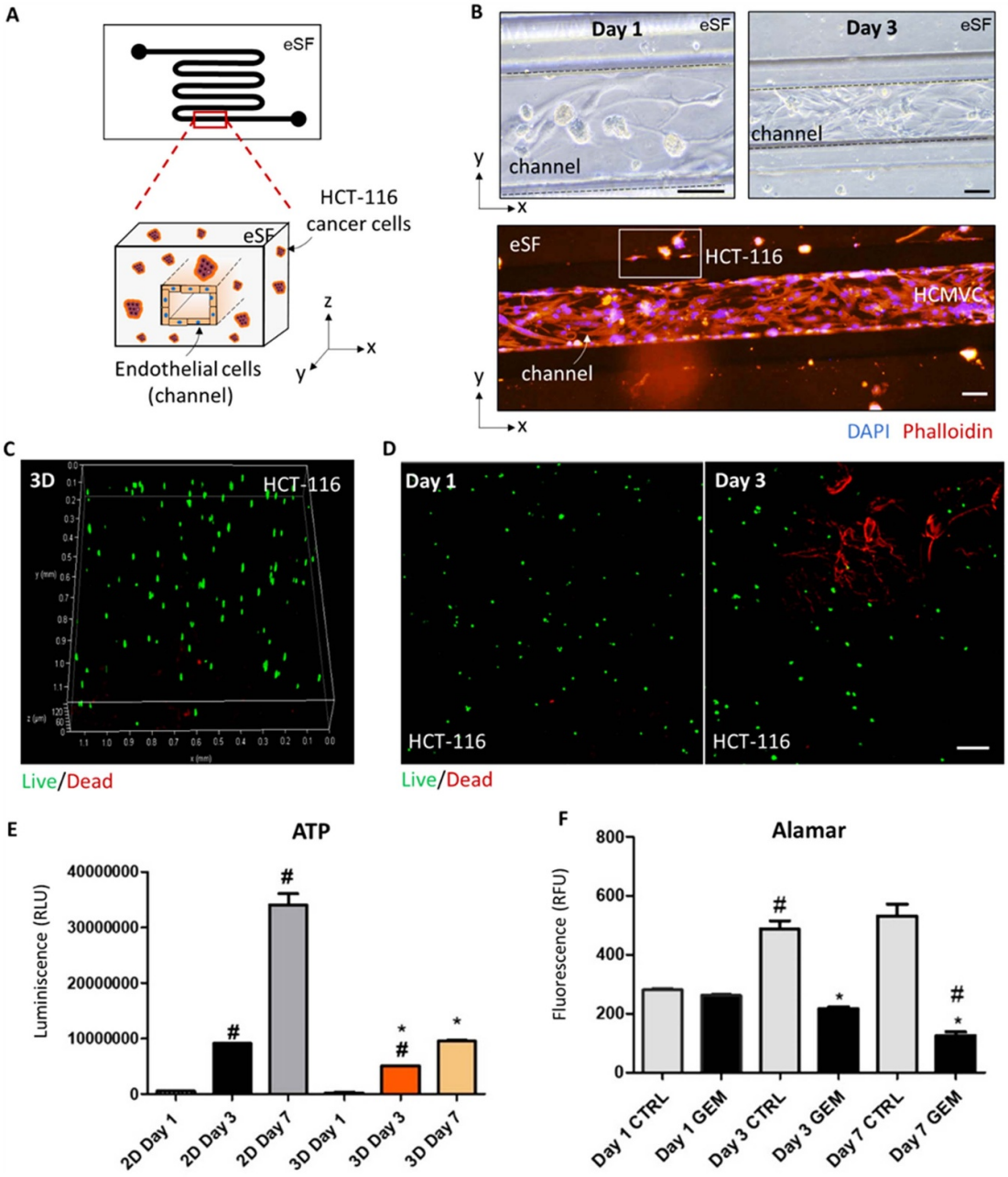


**Figure 4.** CRC eSF microfluidic model. (A) Schematics of the CRC microfluidic model containing endothelial cells seeded on the microchannel and colorectal cancer cells encapsulated throughout the eSF hydrogel. (B) Brightfield images of HCoMECs perfused and adhered in the microchannel on day 1 and day 3; and fluorescence microscopy images of HCoMECs after 5 d of culture (DAPI, blue, nuclei; phalloidin, F-actin, red) showing endothelial cells aligning and creating an endothelialized lumen-like structure within the microchannel. (C) 3D confocal image of a live/dead at day 1. (D) Live/dead assay on days 1 and 3. Live cells are stained in green and dead cells in red. Scale bar: 100 μm. (E) Cell viability studies. ATP quantification graph showing HCT-116 cell metabolic activity in 2D and 3D (encapsulated in eSF hydrogels) cultures after 1, 3 and 7 d of culture. Data are presented as mean ± stdev ($n = 3$), (*) denotes statistical differences in the same day in different conditions ($p < 0.05$), (#) denotes statistical differences within the same state, but compared to timepoint day 1. (F) AB performed in 14% eSF microfluidic platforms with HCT-116 cells encapsulated within, with an 8 μL per hour flow rate of Gemcitabine solution at days 1, 3 and 7. * Significant differences were observed when comparing the control to Gemcitabine (GEM) condition within the same timepoint. # Significant differences when comparing the same situation to the previous timepoint. $p < 0.05$.

normal morphology and elongation 1 d after the seeding. After 3 d, HCoMECS reached a confluent layer characteristic of native vasculature [25]. Finally, due to the hydrogel's high permeability, DAPI/Phalloidin injection also stained HCT-116 located in the bulk of the hydrogels.

*3.4.3. Live/dead assay*

The live/dead assay was performed at a random location of the device on day 1 and day 3 showed that cells were viable and proliferating (figures 4(C) and (D)). This experiment also showed the cells were isotropically distributed across the eSF hydrogel. A significant

statistical difference was found in metabolic activity on days 1 and 3 of culturing, with increased activity on day 3 (figure 4(E)). It showed the ability of the eSF hydrogel microfluidic platform to support a stable and viable culture of HCT-116 cells under perfusion.

*3.4.4. ATP quantification*

We next assessed the viability of HCT-116 cells encapsulated within the 14% eSF hydrogel to determine if the cells survived the fabrication procedure.

To further confirm cell viability, we quantified the levels of ATP both in 2D static and in the eSF microfluidic chip for up to 7 d. A calibration curve was used to define its relationship with bioluminescence in 2D. We performed a direct correlation using the same number of cells to correlate the results in our eSF platform. The signal obtained when testing the hydrogels shows that the cells remained highly viable (figure 4(E)). In 2D, there is a statistical difference in every day within the same timepoint due to cell proliferation in cell flasks without constrains. In 3D, there is only a statistical difference when comparing day 3 and day 1.

*3.4.5. Investigation of the effect of GEM—AB*

The effect of dynamically exposing HCT-116 cells to 5 μM GEM (through the serpentine channel) for the period of 1 d up to 7 d of culturing was investigated. The results obtained from AB assays shows no differences in the presence or absence of GEM on the first day of culture (figure 4(F)). By its turn, it was observed a slight decrease in metabolic activity of cells when cultured in the presence of GEM between day 1 and day 3. This negative effect on cells become more significant after 7 d of culturing.

## 4. Discussion

Hydrogels have been proposed as more relevant materials with the advantage of using the whole three-dimensional hydrogel as a working/testing platform. The material must fulfil several conditions: (i) handle the fabrication methods to make the hydrogel microfluidic device without degenerating; (ii) promote cellular adhesion and homeostasis; (iii) contain chemical groups for hypothetical chemical modification; (iv) exhibit slow or tunable degradation rates for *in vitro* or *in vivo* applications; (v) flexible, but with robust mechanical properties; and (vi) transparent to allow microscope observations.

Herein, we developed a novel method to produce a fully biomimetic microfluidic platform utilizing eSF hydrogel in its amorphous state (resulting from a crosslinking approach proposed by Yan *et al* [19]), showcasing mechanical attributes unattainable through a $\beta$-sheet conformation. The method of fabrication consists in a combination of fabrication techniques, already patented by the group that renders eSF microfluidic platforms in amorphous state [26].

Our group proposed SF hydrogels preparation via a HRP-mediated crosslinking in physiological conditions. In their first systematic study, the authors observed that varied concentrations of SF and HRP/hydrogen peroxide ($H_2O_2$) crosslinking solutions lead to different physicochemical properties of the SF hydrogels, without damaging the cells [27]. This enzymatic crosslinking approach has shown great potential for preparing injectable hydrogels from polymers containing or functionalized with phenol group-containing molecules, including tyrosine, tyramine or aminophenol. It is noteworthy that SF contains 5.3% tyrosine molecules with the required phenol groups.

In this study, we took advantage of our experience with the use of SF in tissue engineering, microfluidics modelling and CRC [14, 23] to design a unique human colorectal tumor model built on the novel soft microfluidic platform. The model was designed to comprise a traditional serpentine channel for HCoMECS seeding, media perfusion, and for the injection of anti-cancer drugs while CRC cells are embedded in the hydrogel (figure 1(A)). The choice of design was made to simply mimic the native tumor environment, which is characterized by displaying a tortuous vasculature.

Regarding the characterization of the 14 wt% silk hydrogel, SEM showed the eSF hydrogel maintained the microfluidic features with excellent fidelity after the entire fabrication process and crosslinking. Since it is not possible to observe wet samples in SEM, the eSF hydrogel microfluidic platform was subjected to critical point drying using $CO_2$. Indeed, this result is of significant importance since hydrogels are mostly made of water and thus may not retain the nano-scaled features required by microfluidics (13). Many hydrogels have been reported in microfluidics, such as collagen [28], gelatin [29] or agarose [30]. However, hydrogels as a base for microfluidics can only work if, after the processing/crosslinking, the microfluidics chambers and channels remain unchanged, with extreme fidelity regarding the mold. This will depend on the inherent features of this type of material, *e.g.* change in size and distortion owed to swelling or drying, that decreases/increases their mechanical properties. Moreover, in some cases, such as Matrigel®, a limited range of stiffness can be achieved that is simply not enough to withstand microfabrication [2].

As of rheology analysis (figure 2(A)), the reported results are in agreement with previous results: The higher the percentage of SF in solution, the stiffer the hydrogel becomes after crosslinking [14]. The ATR-FTIR is used to characterize molecule structure in different samples.

There is an association between hydrogels´ network morphology and conformational changes (detected by ATR-FTIR) of the eSF proteins. When incubating the eSF hydrogel (in PBS at 37 °C), a

relatively transparent morphology is observed over 7 d, starting to change at day 7 to opaque until 10 d [17]. The FTIR-ATR spectra demonstrates that under these conditions, the proteins undergo conformational change—$\beta$-sheet conformation [17, 19]. The cells encapsulated in these hydrogels enter apoptosis due to the stress of protein conformational change. However, if cells are encapsulated on eSF hydrogels already in $\beta$-sheet, cell viability is preserved [17]. This is the reason why our assays only lasted for 7 d. On the other hand, the transparency that the amorphous state of the eSF offer is a must for imaging cell dynamics and viability within the hydrogel.

We next investigated the deformation capacity of the microfluidic chip by performing tensile tests on 14 wt% microfluidic platform (figure 3(C)). The result of 103.96% as mean tensile strength means that the hydrogel can be stretched twice its original size. Altogether, these results demonstrate that the eSF microfluidic platform obtained using this combination of techniques and crosslinking renders a highly elastic platform. To complement the previous assay, we evaluated the capability of the eSF chip to recover to other types of mechanical actuation, namely manual tension, torsion, and bending. As can be seen in figure 3(A), the chip was subject to stretch, bending, and twisting, ever without breaking, and even more importantly, damaging the inner channel. This deformation ability could be optimal in a myriad of tissue models, such as lung, heart and colon, which present dynamic stretching movements [31, 32]. Moreover, this opens the way to deepen mechanobiology studies in the field of cancer.

Media evaporation was prevented in two different ways, just like a normal PDMS microfluidic chip: (1) keeping the chip inside a Petri dish with a few drops of PBS. Before connecting the chip to the pumps, pipette tips with cell media were placed in all inlets and outlets. After connecting the pump, flow rate was kept constant, preventing the endothelial cells from dry out and providing oxygen and nutrients to the encapsulated cancer cells, as was shown by live/dead experiments at day 3.

Regarding the mechanical properties, we know from previous works that SF produced by the method described in this work [19] is obtained in its amorphous state. As the time passes by, around day 7, it starts changing into b-sheet formation, becoming more rigid and opaque. These results on b-sheet and its relationship with mechanical properties have already been published by our group in [33], establishing this trend.

Some concerns were raised due to the hydrophilicity of the material and whether it could perfuse water-based solutions efficiently through the channel. After the injection of a blue ink flowing along the whole serpentine channel was achieved, the ability of the eSF platform to flow fluids has been demonstrated. Moreover, the eSF microfluidic chips are capable of generate molecular gradients as shown in the figure 3(B). The slope of such gradients could be accurately tuned by adjusting the concentration of silk: higher concentrations lead to slower gradient formation due to smaller pore size and lower concentration lead to faster gradient formation due to large pore sizes. Indeed, one of the main properties of eSF is the ease of tuning mechanical stiffness.

Regarding the biological assays, we aimed at building a very simplistic colorectal tumor model. For this, we encapsulated CRC cells (HCT-116) within the bulk of the eSF hydrogel and HCoMECS (microvascular endothelial colonic cells) were seeded in the walls of the serpentine microchannel. We first explored the ability of cells to adhere and spread in the microfluidics channels. Hydrogels obtained from *Bombyx mori* are not utterly absent of binding sequences. Silk proteins contain a main heavy chain, considered a hydrophobic protein with a co-block design [34]. Hydrophilic segments are involved in the self-assembling process, causing differences in water amount and the mechanical properties of the final hydrogel. This can elucidate the mechanisms by which a certain level of cell attachment and migration happens in *Bombyx mori* derived hydrogels [14]. Moreover, sequences that are RGD-like are present in the N-terminal segment of heavy-chain, VTTDSDGNE and NINDFDED [34].

As aforementioned, the proposed SF hydrogels preparation via a HRP-mediated crosslinking in physiological conditions has shown great potential for preparing injectable hydrogels. Indeed, previous works have shown the culture of endothelial cells in eSF hydrogels with good cell adhesion and growth [11]. After seeding endothelial cells in the channels, results of DAPI/Phalloidin staining show normal morphology and elongation. More experiments would be needed to confirm it reached a confluent layer characteristic of native vasculature such as CD31 or VE-Cadherin staining [26, 35]. This makes us feel confident that relevant models for studying cancer and other diseases requiring endothelial vessels could be achieved. Permeability assays were not performed, but the authors feel confident that a cell culture together with pericytes could render a mature blood vessel–like structure.

The viability of HCT-116 cancer cells within the 14 wt% eSF to determine if cells survived the whole fabrication procedure is essential to determine if this novel fabrication technique could be applied in biological studies. The live/dead assay performed at random locations of the device on day 1 and day 3 showed that cells were viable and proliferating (figures 4(C)

and (D)). This experiment also showed the cells were isotropically distributed across the eSF hydrogel.

When analyzing the results of an ATP assay performed on HCT-116 cells in 2D static culture flasks and encapsulated in 3D (eSF microfluidic chip 14%, for 7 d), naturally, cells encapsulated in a rather stiff hydrogels proliferate at lower rates, which was observed. Natural 3D hydrogels confer different characteristics to cells when compared to 2D, such as high cell viability but controlled proliferation and differentiation [36], while in 2D cells grow faster and without physical constrains until they reach confluence. Finally, it is worth noticing the controls, which can provide valuable information about the homeostasis of the cells in the system. This means that the chosen design allows for cell viability: feeding the system through the inlet via the serpentine is enough to provide nutrients/oxygen diffusion to the entire system. These results indicated the ability of the eSF hydrogel microfluidic platform to support a stable and viable culture of HCT-116 cells under perfusion for at least 7 d.

Post-fabrication sterility is assured by sterilization of silk solution under UV-light. Moreover, all the steps since fabrication are done in sterile conditions in a cell biology laboratory. The molds are previously sterilized with ethanol and UV light, and all the procedures from there on are done using sterile materials. There has been a case of contamination inside the silk-microfluidic platform, but the authors were able to trace it back to the initial HCT-116 culture. Media evaporation was prevented in two different ways, just like a normal PDMS microfluidic chip: (1) keeping the chip inside a petri dish with a few drops of PBS. Before connecting the chip to the pumps, pipette tips with cell media were placed in all inlets and outlets. After connecting the pump, flow rate was kept constant, preventing the endothelial cells to dry out and providing oxygen and nutrients to the encapsulated cancer cells, as was shown by live/dead experiments at day 3.

Regarding the mechanical properties, we know from previous works that SF produced by the method described in this work [19] is obtained in its amorphous state. As the time passes by, around day 7, it starts changing into $\beta$-sheet formation, becoming more rigid and opaque. These results on $\beta$-sheet and its relationship with mechanical properties have already been published by our group in [33], establishing this trend.

At last, to complete this soft lab-on-a-chip platform based on eSF hydrogel for colorectal tumor model proof-of-concept, we evaluated the effect of dynamically injecting 5 μM GEM (through the serpentine channel) on HCT-116 cells for up to 7 d [37]. GEM is now being tested as treatment of patients with advanced CRC [38]. AB assays shows no differences in the presence or absence of GEM on the first day of culture, most probably due to the time it takes for the drug to diffuse across the hydrogel and show its effects (figure 4(F)). However, a slight decrease in metabolic activity for GEM between day 1 and day 3 it was observed, being the real antineoplastic effect only observed after 7 d. This 'delay' of cytotoxicity has been shown before, with studies reporting this 'prolonged' effect [39]. Globally, the obtained results (AB and ATP) demonstrated that cells are viable when encapsulated in a highly concentrated mesh of eSF and respond to GEM treatment. Another important aspect to consider when analyzing the data is that, although we were not quantifying and distinguishing cell death among endothelial cells and cancer cells, it is probable that both the cancer cells and the vasculature are sensitive to the treatment since once that the standard-of-care chemotherapeutic GEM also induces secondary effects by not treating just cancer cells. Targeting the nanoparticles towards CRC cells and minimizing deleterious effects on endothelial cells would be very useful and constitute the next step of this work.

In todays' scientific scenario there are more than a few methods to produce a working, *in vivo* like microenvironment. All the methods present its advantages and disadvantages [40]. 3D printing advocates show that inlays for injection molding can be 3D printed, thus reducing the skills, cost, and time required for tool fabrication [41]. Comparing to our method for example, these are not implantable or stretchable, offering a reduced space where the ECM interplay occurs. In brief, we obtained an eSF microfluidic platform that can be used for many biological applications, such as organ-on-chip and point-of-care diagnostics. As an alternative to PDMS, the silk hydrogel can be used since it is cost-effective, and the stiffness can be tailored to the model of choice.

## 5. Conclusion

In this study, we report an advanced and biomimetic microfluidic platform making use of an enzymatically crosslinked eSF hydrogel, by combining photolithography and soft lithography. Functional devices were obtained in amorphous conformation with unique characteristics, such as good malleability, high transparency and flexibility. The SF concentration that presented the best characteristics was 14 wt%, proving that it retains the intricate serpentine features with high level of fidelity. Next, the platform showed a good ability to mimic characteristic features of the native tumor microenvironment, displaying a friendly microenvironment for cells functions as demonstrated by the measured cell viability and metabolic activity. The perfusion of GEM affected cell viability and demonstrated the utility of the developed cell-laden enzymatic-crosslinked SF microfluidic chip to be utilized as a drug screening platform. Importantly, the improvement of soft microfluidics such as the one developed herein

present some important features over the hard microfluidics (PDMS), *e.g.* physiological relevance, functional space, flexibility, ECM interaction analysis, optical properties and easy manipulation. Overall, the developed soft cell-laden eSF hydrogel based microfluidic device may be used in tissue engineering applications, organ or tissue/tumor models, drug discovery/screening, a tissue implant, tissue regeneration or, more interestingly, as implantable and biocompatible microdevices.

## Data availability statement

The data cannot be made publicly available upon publication due to legal restrictions preventing unrestricted public distribution. The data that support the findings of this study are available upon reasonable request from the authors.

## Acknowledgments

The authors acknowledge the financial support provided through the projects PTDC/BTM-ORG/31564/2017, financed by the Portuguese Foundation for Science and Technology (FCT) and cofinanced by European Regional Development Fund (FEDER) and Operational Programme for Competitiveness and Internationalization (POCI). M.R.C. acknowledges her post-doctoral contract TERM RES Hub—Scientific infrastructure for Tissue Engineering and Regenerative Medicine Ref Norte-01-0145-FEDER-02219015 and Portuguese Foundation for Science and Technology (FCT) for the financial support under the CEEC Individual 2021.00049.CEECIND. This work was partially supported by the IET A. F. Harvey Engineering Research Award 2018 (ENG ThE CANCER) and JusThera Project (NORTE-01-0145-FEDER-000055). D.C. acknowledges the Portuguese Foundation for Science and Technology (FCT) for the financial support under the CEEC Individual 2017 (CEECIND/00352/2017) program and the 2MATCH project (PTDC/BTM-ORG/28070/2017). The authors would also like to thank the contributions to this research from the project 'TERM RES Hub—Scientific Infrastructure for Tissue Engineering and Regenerative Medicine', reference PINFRA/22190/2016 (Norte-01-0145-FEDER-022190), funded by the Portuguese National Science Foundation (FCT) in cooperation with the Northern Portugal Regional Coordination and Development Commission (CCDR-N), for providing relevant lab facilities, state-of-the art equipment and highly qualified human resources. The authors thank ONCOSCREEN project funded by the European Union's Horizon Europe research and innovation programme under grant agreement No. 101097036.

## Conflict of interest

The authors declare no conflict of interest.

The authors declare the proposed research does not involve human participants or animal experimentation.

## ORCID iDs

Mariana R Carvalho https://orcid.org/0000-0003-2081-3909
David Caballero https://orcid.org/0000-0001-7930-2535
Subhas C Kundu https://orcid.org/0000-0002-7170-2291
Rui L Reis https://orcid.org/0000-0002-4295-6129
Joaquim M Oliveira https://orcid.org/0000-0001-7052-8837

## References

[1] Preetam S *et al* 2022 Emergence of microfluidics for next generation biomedical devices *Biosens. Bioelectron.* X **10** 100106
[2] Akther F, Little P, Li Z, Nguyen N-T and Ta H T 2020 Hydrogels as artificial matrices for cell seeding in microfluidic devices *RSC Adv.* **10** 43682–703
[3] Morbioli G G, Speller N C and Stockton A M 2020 A practical guide to rapid-prototyping of PDMS-based microfluidic devices: a tutorial *Anal. Chim. Acta* **1135** 150–74
[4] Halldorsson S, Lucumi E, Gómez-Sjöberg R and Fleming R M T 2015 Advantages and challenges of microfluidic cell culture in polydimethylsiloxane devices *Biosens. Bioelectron.* **63** 218–31
[5] Chen M *et al* 2022 Facile microfluidic fabrication of biocompatible hydrogel microspheres in a novel microfluidic device *Molecules* **27** 4013
[6] Buchanan C F, Voigt E E, Szot C S, Freeman J W, Vlachos P P and Rylander M N 2014 Three-dimensional microfluidic collagen hydrogels for investigating flow-mediated tumor-endothelial signaling and vascular organization *Tissue Eng.* C **20** 64–75
[7] Lee Y, Lee J M, Bae P-K, Chung I Y, Chung B H and Chung B G 2015 Photo-crosslinkable hydrogel-based 3D microfluidic culture device: microfluidics and miniaturization *Electrophoresis* **36** 994–1001
[8] Bhusal A, Dogan E, Nguyen H-A, Labutina O, Nieto D, Khademhosseini A and Miri A K 2021 Multi-material digital light processing bioprinting of hydrogel-based microfluidic chips *Biofabrication* **14** 014103
[9] Russo M, Cejas C M and Pitingolo G 2022 Chapter six—advances in microfluidic 3D cell culture for preclinical drug development *Progress in Molecular Biology and Translational Science* ed A Pandya and V Singh (Academic) pp 163–204
[10] Bhusal A, Dogan E, Nieto D, Mousavi Shaegh S A, Cecen B and Miri A K 2022 3D bioprinted hydrogel microfluidic devices for parallel drug screening *ACS Appl. Bio Mater.* **5** 4480–92
[11] Zhao S, Chen Y, Partlow B P, Golding A S, Tseng P, Coburn J, Applegate M B, Moreau J E, Omenetto F G and Kaplan D L 2016 Bio-functionalized silk hydrogel microfluidic systems *Biomaterials* **93** 60–70
[12] Sun W *et al* 2021 Silk fibroin as a functional biomaterial for tissue engineering *Int. J. Mol. Sci.* **22** 1499

[13] Zhang M et al 2019 Printable smart pattern for multifunctional energy-management E-textile *Matter* **1** 168–79
[14] Carvalho M R et al 2018 *Tuning Enzymatically Crosslinked Silk Fibroin Hydrogel Properties for the Development of a Colorectal Cancer Extravasation 3D Model on a Chip* vol 2 (Glob Chall) p 1700100
[15] Carvalho C R, Costa J B, da Silva Morais A, López-Cebral R, Silva-Correia J, Reis R L and Oliveira J M 2018 Tunable enzymatically cross-linked silk fibroin tubular conduits for guided tissue regeneration *Adv. Healthcare. Mater.* **7** e1800186
[16] Bettinger C J, Cyr K, Matsumoto A, Langer R, Borenstein J and Kaplan D 2007 Silk fibroin microfluidic devices *Adv. Mater.* **19** 2847–50
[17] Ribeiro V P et al 2018 Rapidly responsive silk fibroin hydrogels as an artificial matrix for the programmed tumor cells death *PLoS One* **13** e0194441
[18] Costa J, Silva-Correia J, Oliveira J M and Reis R L 2018 *Inks for 3D printing, methods of production and uses thereof* PCT/IB2018/054212 (available at: https://patentscope.wipo.int/search/en/detail.jsf?docId=WO2018225049)
[19] Yan L-P et al 2016 Tumor growth suppression induced by biomimetic silk fibroin hydrogels *Sci. Rep.* **6** 31037
[20] Teixeira L S, Feijen J, van Blitterswijk C A, Dijkstra P J and Karperien M 2012 Enzyme-catalyzed crosslinkable hydrogels: emerging strategies for tissue engineering *Biomaterials* **33** 1281–90
[21] Wen S, Du X, Gou Y and Jiang L 2016 Treatment effects of oxaliplatin combined with gemcitabine on colorectal cancer and its influence on HMGB1 expression *Oncol. Lett.* **12** 3187–90
[22] Maietta I, Martínez-Pérez A, Álvarez R, De Lera Á R, González-Fernández Á and Simón-Vázquez R 2022 Synergistic antitumoral effect of epigenetic inhibitors and gemcitabine in pancreatic cancer cells *Pharmaceuticals* **15** 824
[23] Carvalho M R, Barata D, Teixeira L M, Giselbrecht S, Reis R L, Oliveira J M, Truckenmüller R and Habibovic P 2019 Colorectal tumor-on-a-chip system: a 3D tool for precision onco-nanomedicine *Sci. Adv.* **5** eaaw1317
[24] Carvalho M R, Maia F R, Vieira S, Reis R L and Oliveira J M 2018 Tuning enzymatically crosslinked silk fibroin hydrogel properties for the development of a colorectal cancer extravasation 3D model on a chip *Glob. Challenges* **2** 1700100
[25] Wang X, Phan D T T, Sobrino A, George S C, Hughes C C W and Lee A P 2016 Engineering anastomosis between living capillary networks and endothelial cell-lined microfluidic channels *Lab Chip* **16** 282–90
[26] Carvalho M R et al 2019 Enzymatically crosslinked silk fibroin hydrogel microfluidic platform methods of production and uses thereof
[27] <Deal done over HeLa cell line胞前今生+nature.pdf>
[28] Baker B M, Trappmann B, Stapleton S C, Toro E and Chen C S 2013 Microfluidics embedded within extracellular matrix to define vascular architectures and pattern diffusive gradients *Lab Chip* **13** 3246–52
[29] Treebupachatsakul T, Lochotinunt C, Teechot T, Pensupa N and Pechprasarn S 2022 Gelatin-based microfluidic channel for quantitative E. Coli detection using blue fluorescence of 4-methyl-umbelliferone product and a smartphone camera *IEEE Sens. J.* **22** 12473–84
[30] Li Y, Yan X, Feng X, Wang J, Du W, Wang Y, Chen P, Xiong L and Liu B-F 2014 Agarose-based microfluidic device for point-of-care concentration and detection of pathogen *Anal. Chem.* **86** 10653–9
[31] Kumar V et al 2022 An *in vitro* microfluidic alveolus model to study lung biomechanics *Front. Bioeng. Biotechnol.* **10** 848699
[32] Kitsara M, Kontziampasis D, Agbulut O and Chen Y 2019 Heart on a chip: micro-nanofabrication and microfluidics steering the future of cardiac tissue engineering *Microelectron. Eng.* **203–204** 44–62
[33] Pierantoni L, Brancato V, Costa J B, Kundu S C, Reis R L, Silva-Correia J and Oliveira J M 2023 Synergistic effect of co-culturing breast cancer cells and fibroblasts in the formation of tumoroid clusters and design of *in vitro* 3D models for the testing of anticancer agents *Adv. Biol.* **7** e2200141
[34] Floren M, Migliaresi C and Motta A 2016 Processing techniques and applications of silk hydrogels in bioengineering *J. Funct. Biomater.* **7** 26
[35] Arakelian L et al 2023 Endothelial CD34 expression and regulation of immune cell response *in-vitro Sci. Rep.* **13** 13512
[36] Joseph J S, Malindisa S T and Ntwasa M 2019 Two-dimensional (2D) and three-dimensional (3D) cell culturing in drug discovery *Cell Culture* (IntechOpen) (https://doi.org/10.5772/intechopen.81552)
[37] Cattel L, Airoldi M, Delprino L, Passera R, Milla P and Pedani F 2006 Pharmacokinetic evaluation of gemcitabine and 2′,2′-difluorodeoxycytidine-5′-triphosphate after prolonged infusion in patients affected by different solid tumors *Ann. Oncol.* **17** v142–7
[38] Tefas L R, Barbălată C, Tefas C and Tomuță I 2021 Salinomycin-based drug delivery systems: overcoming the hurdles in cancer therapy *Pharmaceutics* **13** 1120
[39] Toschi L, Finocchiaro G, Bartolini S, Gioia V and Cappuzzo F 2005 Role of gemcitabine in cancer therapy *Future Oncol.* **1** 7–17
[40] Lee Y, Choi J W, Yu J, Park D, Ha J, Son K, Lee S, Chung M, Kim H-Y and Jeon N L 2018 Microfluidics within a well: an injection-molded plastic array 3D culture platform *Lab Chip* **18** 2433–40
[41] Alizadehgiashi M, Gevorkian A, Tebbe M, Seo M, Prince E and Kumacheva E 2018 3D-printed microfluidic devices for materials science *Adv. Mater. Technol.* **3** 1800068